

## Physical mechanisms for tidal dissipation

J.-P. Zahn

*LUTH, Observatoire de Paris, F-92195 Meudon, France*

**Abstract.** A binary system tends to its state of minimum kinetic energy, for given (and conserved) angular momentum : circular orbit, all spins aligned, and rotation of the components synchronized with the orbital motion. The pace at which this final state is achieved depends on the physical processes which are responsible for the dissipation of the kinetic energy. For stars (or planets) with an outer convection zone, the dominant mechanism identified so far is the viscous dissipation acting on the equilibrium tide. For stars with an outer radiation zone, it is the radiative damping operating on the dynamical tide.

I shall review these physical processes, discuss the uncertainties of their present treatment, present the latest developments, and compare the theoretical predictions with the observed properties concerning the orbital circularization of close binaries.

### 1. Introduction

A fundamental property of closed mechanical systems is that they conserve their total momentum. This is true for binary stars, if one ignores the angular momentum which is carried away by winds and by gravitational waves. Through tidal interaction, kinetic energy and angular momentum is exchanged between the two components and their orbit, and due to viscous and radiative dissipation, they evolve to the state of minimum kinetic energy, in which the orbit is circular, the rotation of both stars is synchronized with the orbital motion, and their spin axis are perpendicular to the orbital plane. Whether and how rapidly the system reaches that state is determined by the strength of the tidal interaction, and thus by the separation of the two components. But it also depends on the efficiency of the physical processes which are responsible for the dissipation of the kinetic energy.

Provided these dissipation processes are well enough understood, the observed properties of a binary system can deliver important information on its evolutionary state, on its past history, and even on the conditions of its formation. The first step is thus to identify these physical processes, and it is surprising that this has not been seriously undertaken until the mid-sixties, while tidal theory as such had already reached a high degree of sophistication, starting with the pioneering work of Darwin (1879). In his monumental book, Kopal (1959) states from the onset that he is interested only in “dynamical phenomena which are likely to manifest observable consequences in time intervals of the order of 10 or 100 years, and if so, tidal friction can be safely ignored”.

In contrast, we shall focus here on changes in the properties of binary systems which occur over their evolutionary time scale(s), in particular the circularization of their orbits, which is both easy to observe and easy to interpret. The

first meeting on that subject, whose goal was to bring together observers and theoreticians, was held in 1992 at Bettmeralp (Switzerland); in the preface of the proceedings, A. Duquennoy and M. Mayor remark that the meeting could have been named “the  $e - \log P$  workshop”.

Let us thank Antonio Claret and his colleagues for organizing this new rendez-vous; it revealed to all participants that much progress has been achieved in those 12 years, both in gathering new observational data and in further exploring the relevant physical mechanisms.

## 2. The equilibrium tide

The equilibrium tide assumes that the star is in hydrostatic equilibrium, and that, in the absence of dissipation mechanisms, it would adjust instantaneously to the perturbing force exerted by its companion.

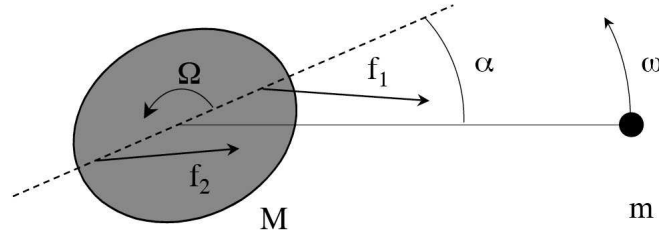


Figure 1. Tidal torque. When the considered star rotates faster than the orbital motion ( $\Omega > \omega$ ), its mass distribution is shifted by an angle  $\alpha$  from the line joining the centers of the two components, due to the dissipation of kinetic energy. Since the forces applied to the tidal bulges are not equal ( $f_1 > f_2$ ), a torque is exerted on the star, which tends to synchronize its rotation with the orbital motion ( $\Omega \rightarrow \omega$ ).

### 2.1. A rough estimate of the tidal torque

Take the system depicted in Fig. 1, of two stars separated by the distance  $d$ , and let us focus on one of the stars that we shall call the primary. Its mass is  $M$  and its radius  $R$ . The companion star of mass  $m$  produces on it two opposite tidal bulges, whose relative elevation  $\delta R/R$  equals approximately the ratio of the differential acceleration exerted on the bulges to the surface gravity  $g$ :

$$\frac{\delta R}{R} \approx \frac{GmR/d^3}{GM/R^2} = \frac{m}{M} \left( \frac{R}{d} \right)^3 \quad (1)$$

( $G$  is the gravitational constant). If the primary star had a constant density, its tidal bulges would have a mass of order  $\delta M \approx (\delta R/R)M$ ; their actual mass is lower, since the surface layers are less dense than the deep interior. These tidal

bulges produce a dipolar gravity field, which causes the motion of the apsides in an elliptic orbit (see Kopal 1959, and P. Smeyers' contribution in this volume).

For simplicity, let us assume that the orbit is circular. When the rotation of the star is synchronized with the orbital motion, the tidal bulges are perfectly aligned with the companion star. However, in the absence of such synchronization, any type of dissipation causes a slight lag of the tidal bulges, and the star then experiences a torque which tends to pull it into synchronism. That torque is easily estimated:

$$\Gamma \approx (f_2 - f_1)R \sin \alpha \approx -\delta M \left( \frac{GmR}{d^3} \right) R \sin \alpha = -\frac{Gm^2}{R} \left( \frac{R}{d} \right)^6 \sin \alpha, \quad (2)$$

where  $\alpha$  is the tidal lag angle, and neglecting numerical factors of order unity.

This angle is a function of the lack of synchronism, and in the simplest case, which is called the *weak friction approximation*, it is proportional to  $(\Omega - \omega)$ ,  $\Omega$  being the rotation rate and  $\omega$  the orbital angular velocity. It also depends on the strength of the physical process which is responsible for the dissipation of kinetic energy, and we may assume that it is inversely proportional to the characteristic time  $t_{\text{diss}}$  of that process. We are thus led to write

$$\alpha \approx \frac{(\Omega - \omega)}{t_{\text{diss}}} \frac{R^3}{GM}, \quad (3)$$

where we have rendered  $\alpha$  non-dimensional by introducing the most “natural” time, namely the dynamical (or free-fall) time  $(GM/R^3)^{-1/2}$ .

From this we can deduce the tidal torque

$$\Gamma \approx -\frac{\Omega - \omega}{t_{\text{diss}}} q^2 M R^2 \left( \frac{R}{d} \right)^6, \quad (4)$$

and the synchronization time  $t_{\text{sync}}$ :

$$\frac{1}{t_{\text{sync}}} = -\frac{1}{(\Omega - \omega)} \frac{d\Omega}{dt} \approx \frac{1}{t_{\text{diss}}} q^2 \frac{M R^2}{I} \left( \frac{R}{d} \right)^6, \quad (5)$$

where  $q = m/M$  is the mass ratio and  $I$  the moment of inertia of the primary star.

## 2.2. Viscous dissipation

In the case of viscous dissipation, the weak friction approximation applies, and the correct expression for the tidal torque, which one derives from the full equations governing the problem, is precisely of the form given above:

$$\Gamma = 6(\Omega - \omega) \frac{\lambda_2}{t_{\text{diss}}} q^2 M R^2 \left( \frac{R}{a} \right)^6; \quad (6)$$

the torque has been averaged here over the orbit, whose semi-major axis is  $a$ . The viscous dissipation time is  $t_{\text{diss}} = R^2 / \langle \nu \rangle$ , where  $\langle \nu \rangle$  is a suitable average of the kinematic viscosity, and  $\lambda_2$  a constant of order unity, which depends on

the mass concentration and on where in the star the tidal torque is applied. For fluid bodies, this torque has been evaluated by Zahn (1966b) and Alexander (1973), assuming uniform rotation.

This expression (6) is valid in the limit of circular orbit; corrections of order  $e^2$  apply when the orbit is elliptic,  $e$  being the eccentricity. Even better, it is possible to derive expressions for the tidal torque which are valid at any  $e$ , as shown by Hut (1981), and Eggleton et al. (1998). As a result, the torque averaged over the elliptic orbit no longer vanishes for  $\Omega = \omega$ , but for

$$\frac{\Omega}{\omega} = \frac{1 + \frac{15}{2}e^2 + \frac{45}{2}e^4 + \frac{5}{16}e^6}{(1 - e^2)^{3/2}(1 + 3e^2 + \frac{3}{8}e^4)}, \quad (7)$$

where *pseudo-synchronization* is achieved.

Since the torque varies along an elliptic orbit, it modifies its eccentricity, as described by

$$\frac{1}{t_{\text{circ}}} = -\frac{d \ln e}{dt} = 3 \left( 18 - 11 \frac{\Omega}{\omega} \right) \frac{\lambda_2}{t_{\text{diss}}} q(1 + q) \left( \frac{R}{a} \right)^8; \quad (8)$$

the companion star contributes a similar amount. Note that synchronization proceeds much faster than circularization, because the angular momentum of the orbit ( $\approx Ma^2\omega$ ) is in general much larger than that stored in the stars ( $I\Omega \ll MR^2\Omega$ ). It was Darwin (1879) who first pointed out that the eccentricity increases when  $\Omega/\omega > 18/11$ .

All these expressions assume implicitly that the angular velocity is constant throughout the star. This is not necessarily the case, since the tidal torque varies with depth, as we shall see, and therefore it tends to impose a state of differential rotation. The problem then becomes much more intricate, since one has to deal in addition with the transport of angular momentum within the star.

Another difficulty arises because such differential rotation modifies the velocity field induced by the tidal force, as was pointed out by Scharlemann (1982); however his treatment is strictly applicable only when the orbit is circular, and it has yet to be extended to elliptic orbits (see the poster by Mathis & Zahn in this volume).

### 2.3. Turbulent convection: the most powerful mechanism for tidal dissipation

In stellar interiors, viscosity due to microscopic processes is very low: it amounts typically to  $\nu \approx 10 - 10^3 \text{ cm}^2\text{s}^{-1}$ . The (global) viscous timescale  $R^2/\nu$  therefore exceeds the age of the Universe.

But viscosity may still play a major role in regions of the star that are turbulent. Then the kinetic energy of large scale flows cascades down to smaller and smaller scales until it is dissipated into heat. The force which acts on the large scale flow may then be ascribed to a “turbulent viscosity” of order  $\nu_t \approx v\ell$ , where  $v$  is the r.m.s. vertical velocity of the turbulent eddies, and  $\ell$  their vertical mean free path.

In stars, the major cause of turbulence is thermal convection, and the magnitude of the turbulent viscosity can be readily estimated using the familiar

mixing-length treatment. When most of the thermal energy is carried by convection, as is the case in late-type main-sequence stars, one finds that the dissipation time-scale is of the order

$$t_{\text{diss}} = t_{\text{conv}} = \left( \frac{MR^2}{L} \right)^{1/3}, \quad (9)$$

where  $L$  is the luminosity of the star. This time is very short, less than 1 year for the Sun, and for this reason turbulent convection is the most powerful dissipation mechanism acting on the equilibrium tide (Zahn 1966b). It works particularly well in stars possessing an outer convection zone, such as solar-type stars. Its effect is considerably reduced in stars with a convective core, as it scales as  $(r_c/R)^7$  with the size  $r_c$  of the core. Furthermore, in such cores the convective turnover time may exceed the tidal period, and therefore the straightforward definition of the turbulent viscosity taken above, i.e.  $\nu_t \approx v\ell$ , can no longer be applied, as we shall see next.

#### 2.4. How to deal with fast tides, or Achilles' heel of tidal theory

When I encountered that problem in my thesis work, I made the straightforward assumption that when the convective turnover time  $t_{\text{conv}} = \ell/v$  exceeds the tidal period  $P_{\text{tide}}$ , the mean free path should be replaced by the distance that turbulent eddies are crossing during, say, half a tidal period. The turbulent viscosity is then given by

$$\nu_t = u\ell \min[1, P_{\text{tide}}/t_{\text{conv}}]. \quad (10)$$

The same problem was tackled somewhat later by Goldreich and Nicholson (1977), when estimating the tidal damping in Jupiter. They remarked that “though the largest convective eddies move across distances of order  $\ell P_{\text{tide}}/t_{\text{conv}}$  in a tidal period, they do not exchange momentum with the mean flow on this time scale”. Assuming that the Kolmogorov spectrum applies to convective turbulence, they retained in that spectrum only the eddies which have a turnover time (or life time) of less a tidal period; in that case, the turbulent viscosity is reduced to

$$\nu_t = u\ell \min[1, (P_{\text{tide}}/t_{\text{conv}})^2]. \quad (11)$$

They concluded that “tidal interactions between Jupiter and its satellites have played a negligible role in the evolution of the latters' orbits”.

Recently Goodman and Oh (1997) proposed yet another scaling, namely

$$\nu_t = u\ell \min[1, (P_{\text{tide}}/t_{\text{conv}})^{5/3}], \quad (12)$$

but after examining the behavior of a dynamical toy model for convection, they concluded that (11) was preferable.

Thus the question of which of these prescriptions should be preferred has still not been settled. One may even question the validity of the very concept of turbulent viscosity, since we know that stratified convection is hardly a diffusive process: the transport of heat and momentum is partly achieved by long-lived plumes, and it is not easy to predict how these will interact with the large

scale tidal flow. But a definite answer may come soon through high resolution numerical simulations of turbulent convection, on which tidal forcing is applied.

Meanwhile we shall present below some observational evidence which indicate that the turbulent viscosity is less drastically reduced than suggested by the second recipe (11).

## 2.5. Beyond the weak friction approximation

When the turbulent viscosity depends on the tidal period, as in the prescriptions presented above, it becomes necessary to break the tidal potential in its Fourier components, and to sum up the torques exerted by each of these. Keeping only the second spherical harmonics of the potential, which is sufficient for most purposes, one has

$$U = \frac{q}{4}\omega^2 r^2 P_2^2(\cos\theta) \sum_l c_l \cos(2\phi - l\omega t), \quad (13)$$

and a similar expression for the axisymmetrical part in  $P_2(\cos\theta)$ . The coefficients  $c_l$  are functions of the eccentricity  $e$ ; to second order in  $e$ , for example, one has

$$c_0 = 0, \quad c_1 = -\frac{1}{2}e, \quad c_2 = 1 - \frac{5}{2}e^2, \quad c_3 = \frac{7}{2}e, \quad c_4 = \frac{17}{2}e^2. \quad (14)$$

In the rotating star, each of these components generates a perturbation of frequency  $(2\Omega - l\omega)$ , which experiences a different turbulent viscosity  $\nu_t$ . This is reflected in the coefficient  $\lambda_2$  introduced above in (6, 8), which takes a different value for each frequency:  $\lambda_{2,l}$ . The equation governing the orbital circularization takes then the following form, to lowest order in  $e$ :

$$\begin{aligned} \frac{d \ln e}{dt} = & -\frac{3}{t_{\text{diss}}} q(1+q) \left(\frac{R}{a}\right)^8 \\ & \left[ \frac{3}{4} \lambda_{0,1} - \frac{1}{8} \lambda_{2,1} \left(1 - 2\frac{\Omega}{\omega}\right) - \lambda_{2,2} \left(1 - \frac{\Omega}{\omega}\right) + \frac{49}{8} \lambda_{2,3} \left(3 - 2\frac{\Omega}{\omega}\right) \right], \end{aligned} \quad (15)$$

where we have added the contribution of the axisymmetrical part of the perturbing potential (the term in  $\lambda_{0,1}$ ). Similar expressions may be derived for the variation of the rotation rate and that of the semi-major axis (see Zahn 1989).

## 3. Comparing with the observations the theory of the equilibrium tide

Having identified the most efficient dissipation mechanism, namely turbulent dissipation acting on the equilibrium tide, we shall now examine how well it accounts for the observed properties in binaries involving at least one component possessing an outer convection zone. We shall treat in turn the case of solar-type binaries on the main-sequence, that of such binaries during their pre-main sequence phase, and finally that of binaries in which one component has evolved to the giant branch.

### 3.1. Solar-type binaries on the main sequence

Applying eq. (8) to a binary of equal components, and of age  $t_{\text{age}}$ , one finds that its orbit should be circular if its period is less than about

$$P_{\text{circ}} = 6 \left( \frac{t_{\text{age}}}{5 \text{ Gyrs}} \right)^{3/16} \text{ days.} \quad (16)$$

To obtain this result we assumed that the rotation was synchronized with the orbital motion, and that the eccentricity decreased from  $e = 0.30$ , a typical value for non-circularized binaries, to  $e = 0.02$ , taken as detectability threshold for circularization. (If one takes this threshold to be  $e = 0.05$ , the circularization period increases to 6.92 days for 5 Gyrs.)

Koch and Hrivnak (1981) were the first to compare this theoretical prediction with the distribution  $e(P)$  of field binaries drawn from Batten's catalogue, and they found them to be compatible, although the critical period  $P_{\text{circ}}$  was rather poorly defined, as one may expect with such a heterogeneous sample of stars of different ages.

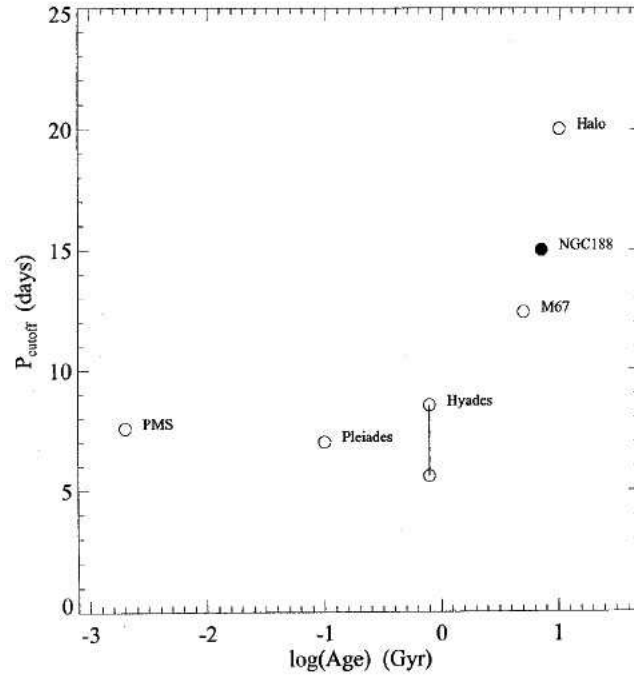


Figure 2. Critical circularization cutoff period vs. age for six coeval stellar samples: PMS (Melo et al. 2001), Pleiades (Mermilliod et al. 1992), Hyades (Duquennoy et al. 1992), M67 (Latham et al. 1992), NGC 188 (Mathieu et al. 2004) and Galactic halo stars (Latham et al. 1992). Note the near constancy of this period below 1 Gyr, at about  $P_{\text{cutoff}} \approx 8$  days, and its increase with age beyond. (From Mathieu et al. 2004; courtesy ApJ.)

But the fact that the critical period is a slowly increasing function of age should be observable, by examining the properties of coeval cluster binaries. Mathieu and Mazeh (1988) found indeed such a trend, when they compared the critical period of different clusters, and they suggested that the measure of  $P_{\text{circ}}$  could serve to evaluate the age of a cluster. However for M67, a cluster of about solar age, they found that the critical period was located between 10,3 and 11 days, well above the predicted 6 days, meaning that tidal dissipation was about 20 times more efficient than inferred from the mixing-length theory.

A recent update was recently made by Mathieu et al. (2004); it summarizes the beautiful work accomplished over more than a decade by several dedicated teams (Fig. 2). As discussed by B. Mathieu in these proceedings, it shows that the cutoff period for circularization increases with age beyond 1 Gyr, but that it is constant below, at  $P_{\text{cutoff}} \approx 7 - 8$  days. It thus appears that two different mechanisms are at work, one operating on old binaries, and another which circularizes the young binaries. In fact, the latter had already been identified some time before.

### 3.2. Circularization during the pre-main-sequence phase

Since orbital circularization depends so strongly on the radius of the star: according to (8)  $-d \ln e / dt \propto R^8$ , one expects much of that circularization should occur on the PMS, where the stellar radius can easily be 5 times larger than on the main-sequence. Following this remark first made by Mayor and Mermilliod (1984), I undertook with L. Bouchet to integrate the equations describing the tidal evolution of solar-type binaries, starting from the birthline defined by Stahler (1983, 1988). Since on the PMS the convective turnover time can exceed the orbital period, it will also exceed the period of most Fourier components present in the tidal perturbation (cf. 13), and therefore one must take into account the reduction of the turbulent viscosity, as discussed in §(2.5.).

The result is depicted in Fig. 3, for a binary consisting of two solar-mass stars. The initial conditions were taken as  $R = 4.79R_{\odot}$ ,  $e = 0.3$ ,  $(\Omega/\omega) = 3$ , and the orbital period  $P$  was chosen such that the eccentricity would drop to 0.005 when the binary reaches the zero age main-sequence (ZAMS). The rotation quickly synchronizes with the orbital motion (in less than  $10^5$  yrs), but thereafter the tidal torque weakens because the convection zone retreats, while the star keeps contracting; therefore the rotation speeds up again to about  $(\Omega/\omega) = 2$  at the ZAMS. Once the star has settled on the MS, synchronization resumes, and is complete by an age of 1 Gyr. The eccentricity first increases, as long as  $(\Omega/\omega) > 18/11$ , and then it steadily decreases to reach its final value  $e = 0.005$  at the ZAMS. Little circularization occurs later on the MS. Angular momentum is transferred to the orbit, which explains why the period increases from 5 to 7.8 days. This final period depends little on the mass of the components, and it is thus the cutoff period for circularization, in the absence of other tidal braking mechanism.

This cutoff period agrees remarkably well with the properties of late type binaries younger than 1 Gyr, and thus there is little doubt that the circularization in these stars is due to the action of the equilibrium tide on the PMS. The main uncertainties in the theoretical prediction are the initial radius  $R_i$  ( $P_{\text{cutoff}}$  scales as  $R_i^{15/16}$ ) and the prescription used to reduce the turbulent vis-



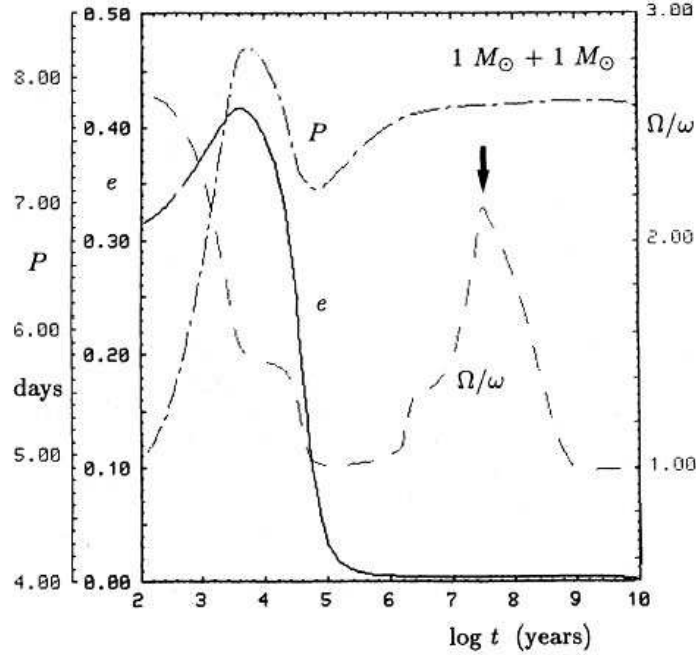


Figure 3. Evolution in time of the eccentricity  $e$ , the orbital period  $P$  and of the ratio between rotational and orbital frequencies ( $\Omega/\omega$ ), for a system with two components of  $1 M_{\odot}$ . The initial period has been chosen such that the eccentricity would decrease from 0.300 to 0.005 when the binary reaches the zero age main-sequence (indicated by an arrow). (From Zahn & Bouchet 1989; courtesy A&A.)

cosity when the tidal period becomes shorter than the convective turnover time. We took here the linear prescription (10); with the other, quadratic prescription (11) the predicted cutoff period would be substantially shorter, contrary to what is observed.

### 3.3. Circularization of binaries evolving off the main-sequence

As another test for the tidal theory, Verbunt and Phinney (1995) chose wide binaries containing giant stars, because they avoid what they call the “troublesome problem of pre-main sequence circularization” we just discussed, and because in such binaries the tidal period exceeds the convective turnover time, so that there is no need to worry about reducing the turbulent viscosity.

They selected 29 binaries with giant components in several galactic clusters, whose age and distance are well established. They integrated the circularization equation (8) for these binaries from the MS to their present location in the HR diagram, and cast the result in the form  $-\Delta \ln e/f$ , where  $-\Delta \ln e$  is the change in eccentricity, and  $f$  a factor which depends on the convection theory used to calculate the turbulent dissipation. For the classical mixing-length treatment that was employed in §2.3.,  $f = 1.01(\alpha/2)^{4/3}$  (Zahn 1989),  $\alpha$  being the ratio

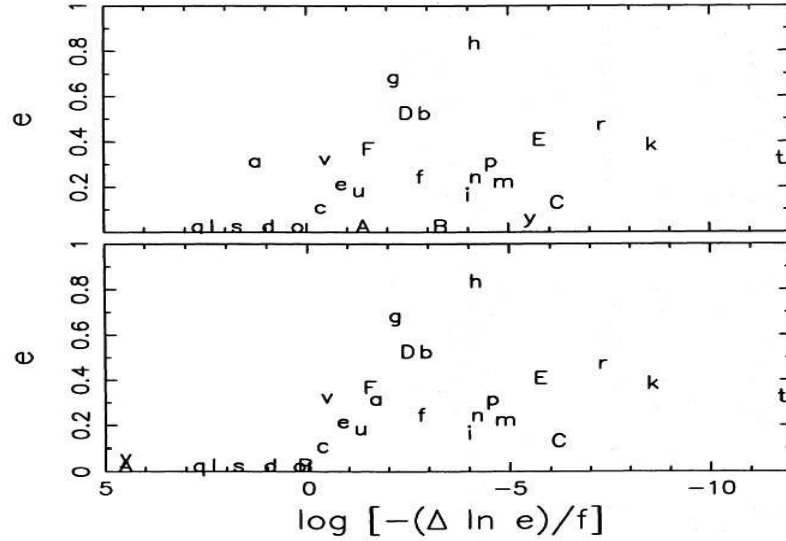


Figure 4. Observed eccentricities of binaries including a giant component vs. the change in excentricity predicted by the tidal theory, invoking the equilibrium tide with turbulent dissipation in the convection zone (Verbunt & Phinney 1995; courtesy A&A). In the upper panel the giant component is assumed to be on the asymptotic giant branch; some corrections have been applied to obtain the result of the lower panel (see text).

of the mixing-length to the pressure scale-height, and therefore  $f$  should be of order unity.

Fig. 4 displays the observed eccentricity of these binaries (each individually labeled by a letter) as a function of the predicted drop in eccentricity  $-\Delta \ln e$ , or rather  $\log[-\Delta \ln e/f]$ . For  $-\Delta \ln e/f > 1$  (i.e.  $-\log[-\Delta \ln e/f] < 0$ ), the orbit should be circularized, whereas it should not for  $-\log[-\Delta \ln e/f] > 0$ . Phinney and Verbunt assume that all binaries are presently on the asymptotic giant branch (core helium burning), because they stay there 10 times longer than on the red giant branch (shell hydrogen burning).

The result is shown in the upper panel: the great majority of binaries complies with the theoretical prediction, but there are 4 exceptions: binary ‘a’ has kept an eccentricity of 0.30, while its orbit should be circular, and binaries ‘A’, ‘B’, ‘y’ have circular orbits, where they should be elliptic. Phinney and Verbunt concluded that binary ‘a’ must still be ascending the red giant branch, and that the other 3 binaries must have undergone an exchange of matter, which very efficiently circularizes the orbit, and therefore that they should have an evolved companion, such as a white dwarf. After these adjustments, the 4 binaries are then no longer exceptions, as can be seen in the lower panel; moreover, the fact that the transition from circular to elliptic orbits occurs in the vicinity of  $\log[-\Delta \ln e/f] \approx 0$  confirms that the parameter  $f$  is indeed of order unity, thus validating the theory of the equilibrium tide with turbulent dissipation.

Two years later Landsman et al. (1997) announced that the secondary of S1040 in M67, the binary labeled ‘A’, is indeed a white dwarf, as was brilliantly conjectured by Verbunt and Phinney.

We may thus conclude that turbulent viscosity acting on the equilibrium tide explains most observations, with the important exception of the circularization of main-sequence binaries older than about 1 Gyr, for which it seems that we have to seek another dissipation mechanism.

#### 4. The dynamical tide

Due to its elastic properties, a star can oscillate in various modes: acoustic modes, internal gravity modes, inertial modes, where the restoring force is respectively the compressibility of the gas, the buoyancy force in stably stratified regions, and the Coriolis force in the rotating star. If their frequency is low enough, these modes can be excited by the periodic tidal potential; the response is called the *dynamical tide*.

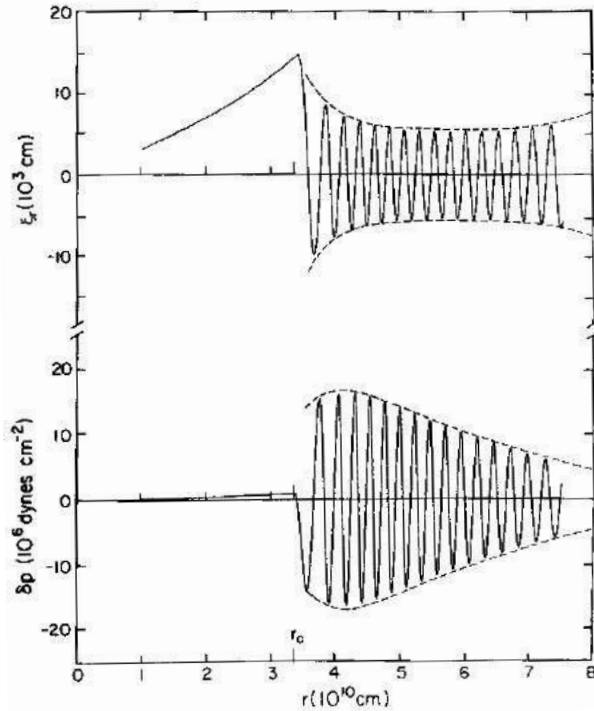


Figure 5. Gravity mode in a  $5 M_{\odot}$  main sequence star excited by a tidal potential of frequency  $\sigma = 2 \cdot 10^{-5} \text{ s}^{-1}$ :  $\xi_r$  is the radial displacement, and  $\delta p$  the pressure perturbation. The radius of the star is  $1.88 \cdot 10^{11} \text{ cm}$ ; only the inner region is shown here (from Goldreich & Nicholson 1989; courtesy ApJ).

##### 4.1. Gravity modes excited by a tidal potential

The modes which have received most attention so far are the tidally excited gravity modes; associated with radiative damping, they have first been invoked for the tidal evolution of massive main-sequence stars (Zahn 1975). Their restoring

force is provided by the buoyancy, whose strength is measured by the buoyancy frequency  $N$ , with

$$N^2 = \frac{g}{H_P} \left[ \delta \left( \frac{\partial \ln T}{\partial \ln P} \right)_{\text{ad}} - \frac{d \ln T}{d \ln P} + \varphi \frac{d \ln \mu}{d \ln P} \right], \quad (17)$$

using classical notations, and  $\mu$  being the molecular weight ( $\delta = -\partial \ln \rho / \partial \ln P$  and  $\varphi = \partial \ln \rho / \partial \ln \mu$  are unity for perfect gas).

The modes which are most excited are those whose frequency is close to the tidal frequency, and these are of high radial order: typically they have more than 10 or 20 radial nodes in the radiation zone, because their wavelength scales as  $\lambda_r \propto r\sigma/N$ , and because the tidal frequency  $\sigma$ , measured in  $\text{days}^{-1}$ , is much lower than the buoyancy frequency  $N$ , measured in  $\text{hours}^{-1}$ . See Fig. 5 for a typical example of such modes, in a  $5 M_\odot$  ZAMS star. Dissipation has been neglected, and therefore the mode is an adiabatic standing wave; note that it is evanescent in the convective core.

These gravity modes couple with the exciting potential in the vicinity of the convective core, whereas their damping occurs mainly near the surface, because the thermal damping time is much shorter there than in the deep interior. The angular momentum drawn from the orbit is deposited near the surface, and hence it is the surface layers which are synchronized first with the orbital motion. As was emphasized by Goldreich and Nicholson (1989), this synchronization is further sped up because the local tidal frequency experienced by the fluid particles entrained by the differential rotation,  $\sigma = 2(\Omega(r) - \omega)$ , tends to zero, and so does also the radial wavelength  $\lambda_r$ , as we seen above, thus enhancing the damping.

For low enough tidal frequency, the tidal wave is completely damped (meaning that it has become a pure propagating wave)<sup>1</sup>, and one can use the WKB treatment to evaluate the total torque applied on the star (Zahn 1975). For the synchronization time (assuming uniform rotation) one finds

$$\frac{1}{t_{\text{sync}}} = -\frac{d}{dt} \left| \frac{2(\Omega - \omega)}{\omega} \right|^{-5/3} = 5 \left( \frac{GM}{R^3} \right)^{1/2} q^2 (1+q)^{5/6} \frac{MR^2}{I} E_2 \left( \frac{R}{a} \right)^{17/2}, \quad (18)$$

and likewise for the circularization time, assuming that synchronization has been quickly achieved:

$$\frac{1}{t_{\text{circ}}} = -\frac{d \ln e}{dt} = \frac{21}{2} \left( \frac{GM}{R^3} \right)^{1/2} q(1+q)^{11/6} E_2 \left( \frac{R}{a} \right)^{21/2}; \quad (19)$$

the companion star contributes a similar amount.  $E_2$  is a constant measuring the coupling between the tidal potential and the gravity mode, and that is why it depends sensitively on the size of the convective core. It has been tabulated by Claret and Cunha (1997) for various stellar models; for a  $10 M_\odot$  ZAMS star, it is  $E_2 \approx 10^{-6}$ .

---

<sup>1</sup>Note that this property of complete damping cannot be captured in the quasi-adiabatic approximation which was used recently by Willems et al. (2003).

This theory was initially developed for pure gravity modes, and as such it was strictly applicable only to non-rotating stars. It was later extended by Rocca (1989) to (uniformly) rotating stars; she showed that taking the Coriolis force into account modifies only slightly the results presented above.

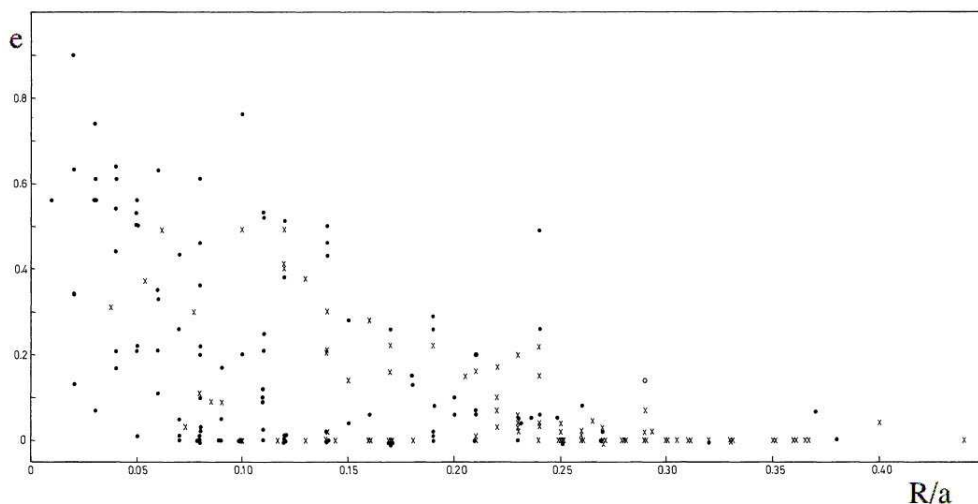


Figure 6. Eccentricity  $e$  vs. fractional radius  $R/a$  for early-type binaries (spectral types O, B, F) listed in Batten's catalogue (from Giuricin et al. 1984; courtesy A&A).

#### 4.2. Circularization of early-type binaries

Giuricin et al. (1984) were the first to compare the predictions of tidal theory with the properties of early-type binaries. Applied to binaries with two identical components of mass between 2 and 15  $M_{\odot}$ , eq. (19) predicts a cutoff value of  $R/a \approx 0.25$  for the fractional radius, i.e. the radius expressed in units of semi-major axis<sup>2</sup>. This value is in good agreement with the observed distribution of eccentricities vs. fractional radius displayed in Fig. 6, although many binaries are circular for  $R/a < 0.25$ .

A similar investigation was recently carried out on eclipsing binaries which had been detected in the Magellanic Clouds during the MACHO and OGLE campaigns (North & Zahn 2003). The results are shown in Fig. 7. Here again the  $e$  vs.  $R/a$  distribution strongly suggests a cutoff value of  $R/a = 0.255$ , in excellent agreement with theory, but an important fraction of binaries are circular at lower fractional radius. It is as if there were two population of binaries, one complying with the predictions above, and the other experiencing

---

<sup>2</sup>This value depends little on mass (Zahn 1977); translated into tidal periods, the cutoff periods would spread between 1 to 2 days, which explains why it is preferable to use  $R/a$  for the observational test.

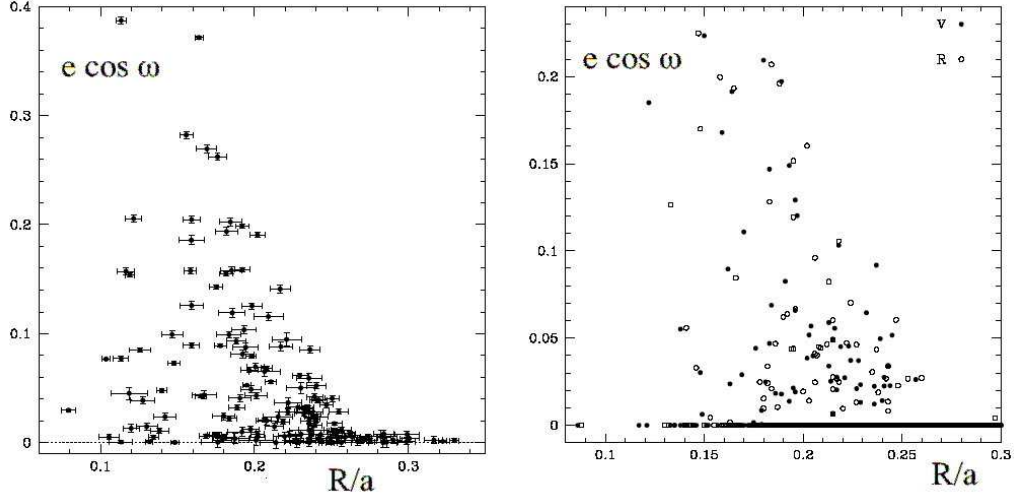


Figure 7. Left panel:  $e \cos \omega$  vs. relative radius  $R/a$  for detached eclipsing binaries in the SMC. Right panel: same for the LMC, full dots based on V lightcurves, open dots based on R lightcurves. (From North & Zahn 2003; courtesy A&A.)

another, more efficient tidal damping. Histograms of the eccentricity distribution at given  $R/a$  confirm that impression.

One may wonder why the binaries in the Magellanic Clouds behave so similarly to those in our Galaxy: they have lower metallicities, and therefore somewhat larger convective cores, and one would expect that these differences be reflected in the coefficient  $E_2$ . However the radii differ too, and the two effects compensate each other such that the predicted cutoff periods are very nearly the same.

#### 4.3. Resonance locking in early-type binaries

Recently Witte and Savonije (1999a, 1999b) revisited the theory of the dynamical tide, by making full account of the Coriolis force, while still neglecting the effect of the centrifugal force. Instead of projecting the forced oscillations on spherical functions, they solved the governing equations directly in two dimensions  $(r, \theta)$ , for several values of the angular velocity  $\Omega$  and of the tidal frequency  $\bar{\sigma} = \sigma - 2\Omega$  in the rotating frame. Let us recall that  $\sigma = 2\omega$  in a circular orbit, but that in an elliptic orbit many more tidal frequencies appear:  $\sigma = \omega, 3\omega$  etc. (see §2.5.).

The result is displayed in Fig. 8 for a star rotating at 20% of the breakup velocity:  $\Omega = 0.2\Omega_c$  (at  $\Omega_c$  gravity is balanced exactly by the centrifugal force at equator); an interpolating curve has been fitted through the calculated points. When the orbit is circular and the star rotates in the same sense as the orbital motion, only one retrograde mode can be excited at  $\bar{\sigma} = 2(\omega - \Omega)$ . But when the orbit is elliptic, many other tidal frequencies appear:  $\bar{\sigma}_l = l\omega - 2\Omega$ , and both retrograde and prograde modes can be excited. One sees that it is very likely that a binary undergoes some resonances during its evolution, both because

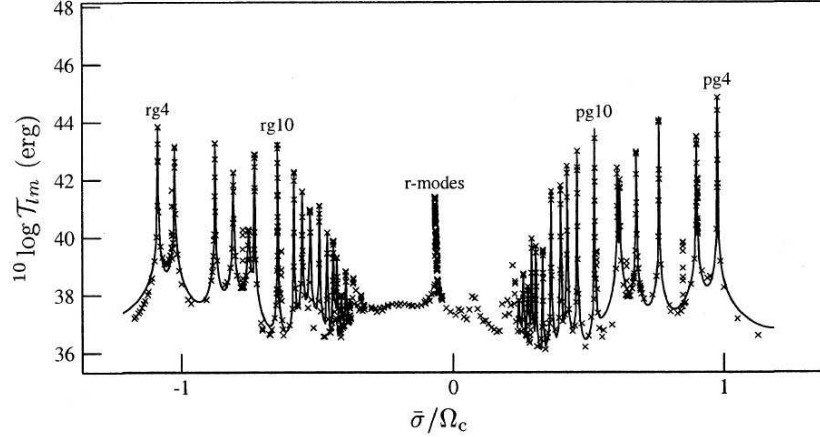


Figure 8. Tidal torque as a function of tidal frequency  $\bar{\sigma} = (l\omega - 2\Omega)$  normalized by the angular breakup velocity  $\Omega_c$ , in a  $10 M_\odot$  star. The star rotates at 20% of the breakup speed. The labels r, pg and rg refer respectively to r-modes, and to prograde and retrograde gravity modes. (From Witte & Savonije 1999a; courtesy A&A.)

the tidal frequency shifts in the course of synchronization, and because the eigenfrequencies are affected by the structural changes of the stars.

The effect of resonances on tidal evolution was largely ignored earlier (Zahn 1975; Rocca 1989; Goldreich & Nicholson 1989) on the grounds that stars would move quickly through such resonances, because their width  $\Delta\sigma$  is inversely proportional to their amplitude. But, most interestingly, Witte and Savonije (1999b) showed that this is not necessarily true, and that a binary can be trapped into a resonance, when one takes into account the whole set of tidal frequencies associated with an elliptic orbit. Retrograde and prograde modes exert torques of opposite sign on the star, and they may lock it into such resonances. Moreover, structural changes also can conspire to favor such locking. The consequence is that circularization is sped up by such resonances, as demonstrated by several specific cases they have studied. These cases are rather sensitive to the initial conditions, which may explain the observational result mentioned above that for the same orbital period (or fractional radius), some binaries are circular while the others are not, as if there were two tidal damping mechanisms.

Recently Willems et al. (2003) too examined the behavior of a  $5 M_\odot$  binary in the vicinity of resonances, using the quasi-adiabatic approximation; however they did not include the Coriolis force, which according to Witte and Savonije plays an important role in coupling the eigenmodes.

#### 4.4. Resonance locking in late-type binaries

Let us come back to the late-type main-sequence binaries. We have seen that turbulent dissipation of the equilibrium tide, at least in its present state, cannot explain the circularization observed in binaries older than 1 Gyr. This incited

Terquem et al. (1998), and almost at the same time Goodman and Dikson (1998), to examine whether the dynamical tide could not be responsible for the observed circularization. Both teams invoked radiative damping as dissipation mechanism, as had been done previously for early-type stars. But here such damping is rather weak, because the oscillation modes are evanescent in the convection zone, where thermal dissipation is strongest. Therefore, contrary to what has been found in early type stars, oscillations modes can enter in resonance at very low tidal frequency, i.e. very close to synchronization. This means that one has to deal with modes which have up to thousand radial nodes, which puts a serious burden on the numerical work, as experienced by Terquem et al.; they restricted their exploration to the vicinity of 3 orbital periods, but included turbulent dissipation in the convection zone, where the modes are evanescent. On the contrary, Goodman and Dikson chose a semi-analytical WKB approach, much as in Zahn (1977).

Though their quantitative results differ somewhat, the conclusions of the two teams agree, namely that the dynamical tide cannot account for the circularization of the oldest late-type binaries; comparing the predicted cutoff periods, one sees that it is less efficient than the equilibrium tide.

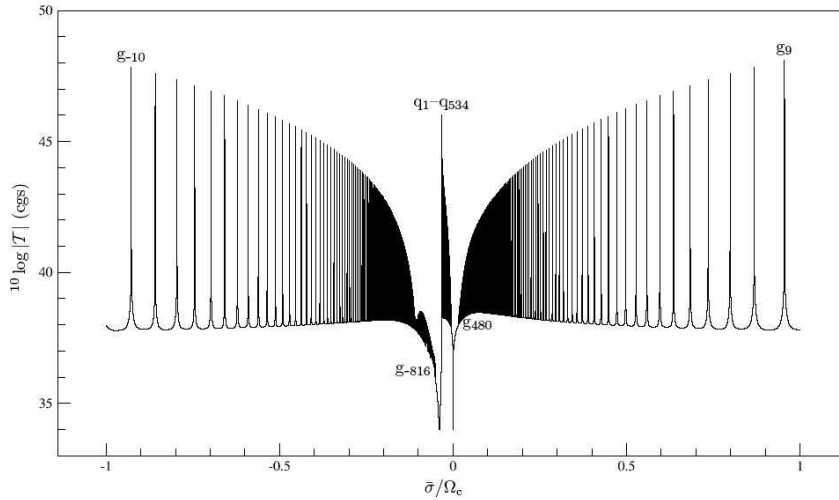


Figure 9. Torque integral vs. tidal frequency  $\bar{\sigma}$  for a  $1 M_{\odot}$  star evolved to the point where the central hydrogen abundance  $X_c = 0.4$ . Results are for a fixed fractional radius  $R/a = 0.25$  and for a companion of  $1 M_{\odot}$ . (From Savonije & Witte 2002; courtesy A&A.)

The problem was re-examined shortly after by Witte and Savonije (2002), who anticipated that here also resonance locking could play an important role. They made account of the Coriolis force, but refrained from the direct 2D calculations they used for early-type binaries, which would be much more cumbersome given the high order of the modes. Instead, they retained only the radial component of the rotation vector, in the so-called “traditional approximation” (which is justified in the limit of low exciting frequency). The  $r$  and  $\theta$  variables then



separate again, as in the non-rotating case, but the horizontal functions are no longer the spherical harmonics (Savonije & Witte 2002).

Fig. 9 displays the tidal torque as a function of the tidal frequency; it illustrates how dense the frequency spectrum is, and how likely resonances may occur as the star sweeps through this graph. Witte and Savonije followed the dynamical evolution of selected binaries given initial conditions for the eccentricity, the orbital period and the rotation rate. For instance, starting with an orbital period of 16 days, they found that the eccentricity decreases from 0.6 to less than 0.01 in a MS life time.

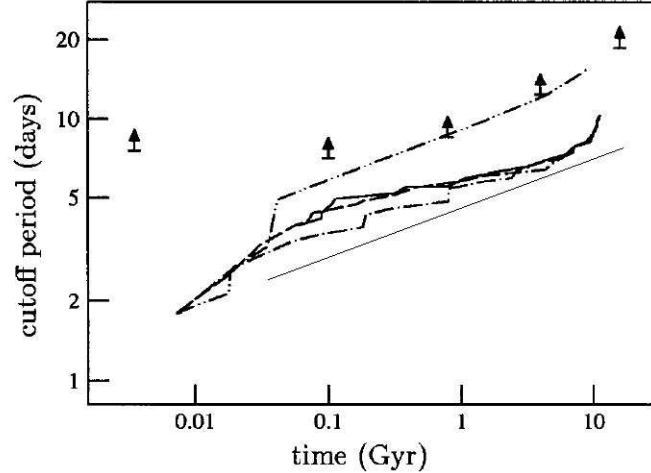


Figure 10. Comparison of observed circularization cutoff periods (arrows) with the theoretical predictions of the equilibrium tide (Zahn 1977) in fine continuous line, and those of the dynamical tide including resonance locking (Witte & Savonije 2002). The latter depend on the initial conditions: the upper dash-dot-dot curve designates binaries with initially very slowly rotating stars (period 100 days), the other three refer to supersynchronous or quasi-synchronous stars (adapted from Witte & Savonije 2002; courtesy A&A.)

Today this process of resonance locking in the dynamical tide thus appears as the most efficient, *on the main-sequence*, among all dissipation mechanisms which have been explored, as is demonstrated in Fig. 10. When starting with quasi-synchronous or super-synchronous stars, the predicted cut-off period is a slowly increasing function of age; for  $5 \cdot 10^9$  yrs, this period is about 7 days, thus higher than that predicted by the equilibrium tide (6 days). But even so, the theoretical points are well below the observed ones, unless one allows for very slow, and rather unrealistic initial rotation (period of 100 days). Let us recall that below 1 Gyr the observations agree very well with the cutoff period derived for the PMS circularization through the equilibrium tide, as we have seen in §3.2.

## 5. Conclusion and perspectives

Let me summarize. The two tidal dissipation processes which have received most attention so far, namely turbulent dissipation of the equilibrium tide and radiative damping of the dynamical tide, have been quite successful in explaining the observed orbital circularization of binary stars. This is particularly true for the early-type MS stars, whose cutoff period agrees extremely well with that predicted by the theory of the dynamical tide, which is thus validated. However many of such binaries are circularized well above this cutoff period, as if they had experienced another, more efficient tidal dissipation mechanism, yet to be identified. But a very likely explanation for this behavior is that these binaries have undergone several episodes of resonance locking, as was described by Witte and Savonije (1999a, 1999b).

The equilibrium tide with turbulent dissipation accounts very well for the properties of binaries containing a red giant, as was demonstrated by Verbunt & Phinney (1995). It also explains the cutoff period of about 8 days observed in late-type binaries younger than about 1 Gyr: these have been circularized during the PMS phase, when they were much more voluminous and fully convective. The only serious discrepancy seems to be the behavior of late-type main-sequence binaries older than 1 Gyr, whose cutoff period increases with age and is higher than that predicted when applying straightforward the theory of the equilibrium tide<sup>3</sup>. Here again one may invoke the dynamical tide with resonance locking, as was shown by Witte and Savonije (2002).

Their mechanism appears thus highly promising, and it ought to be further explored. For instance, one should take into account that the tidal torque is applied primarily to specific regions: the outer convection zone in late-type MS stars and the outermost part of the radiation zone in early-type stars. These regions are synchronized more quickly than the rest of the star, and therefore differential rotation develops in their radiation zone. This increases the radiative damping, since the local tidal frequency tends then to zero as the tidal wave approaches the synchronized region, as we explained in §4.1.

Work is in progress on several other points, and I shall quote only a few. Kumar and Goodman (1996) have studied the enhanced damping of the oscillations triggered in tidal-capture binaries, due to non-linear coupling between the eigenmodes, which is extremely strong in such highly eccentric orbits. Rieutord (2004) is examining the possibility that the so-called elliptic instability may occur in binary stars; this instability is observed in the laboratory when fluid is forced to rotate between boundaries that have a slight ellipticity, and it leads to turbulence. Even the equilibrium tide is being revisited, when applied to a differentially rotating convection zone, as we have already mentioned (see the poster by Mathis & Zahn in this volume).

Finally, the reader may have noticed that I made no attempt here to reconcile the theoretical predictions for the synchronization of the binary components with their observed surface rotation. The reason is that in most cases the tidal torque is applied mainly to the surface layers, which are synchronized much more rapidly

---

<sup>3</sup>The situation has thus improved since the Bettmeralp meeting, where it was felt that the PMS binaries were discrepant too.

than the interior; therefore the interpretation of the surface rotation requires to model the transport of angular momentum within the radiation zone, a difficult task which has not been seriously undertaken so far. But I am confident that we will see progress in solving this problem when we meet again the next time, hopefully in a not too distant future!

**Acknowledgments.** I wish again to express my warm thanks to Antonio Claret and his colleagues of the IAA for organizing this very stimulating meeting. This work was supported by the Centre National de la Recherche Scientifique (Programme de Physique Stellaire).

## References

- Alexander, M.E. 1973, *Ap&SS*, 23, 459  
 Claret, A., & Cunha, N.C.S. 1997, *A&A*, 318, 187  
 Darwin, G.H. 1879, *Phil. Trans. Roy. Soc.*, 170, 1  
 Eggleton, P.P., Kiseleva, L.G., & Hut, P. 1998, *ApJ*, 499, 853  
 Giuricin, G., Mardirossian, F., & Mezzetti, M. 1984, *A&A*, 134, 365  
 Goldreich, P., & Keeley, D.A. 1977, *ApJ*, 211, 934  
 Goldreich, P., & Nicholson, P.D. 1989, *ApJ*, 342, 1079  
 Goodman, J., & Dickson, E.S. 1998, *ApJ*, 507, 938  
 Goodman, J., & Oh, S.P. 1997, *ApJ*, 486, 403  
 Hut, P. 1981, *A&A*, 99, 126  
 Koch, R.H., & Hrivnak, B.J. 1981, *AJ*, 86, 438  
 Kopal, Z. 1959, *Close binary systems*, ed. Chapman & Hall, London  
 Kumar, P., & Goodman, J. 1996, *ApJ*, 466, 946  
 Landsman, W., Aparicio, J., Bergeron, P., Di Stefano, R., & Stecher, T.P. 1997, *ApJ*, 481, L93  
 Latham, D.W., Stefanik, R.P., Torres, G., Davis, R.J., Mazeh, T., Carney, B.W., Laird, J.P., & Morse, J.A. 2002, *AJ*, 124, 1144  
 Mathieu, R.D., & Mazeh, T. 1988, *ApJ*, 326, 256  
 Mathieu, R.D., Meibom, S., & Dolan, C. 2004, *ApJ*, 602, 121  
 Mayor, M., & Mermilliod, J.-C. 1984, *Observational Tests of the Stellar Evolution Theory (IAU Symp. 105)*, ed. A. Maeder & A. Renzini, 411  
 Melo, C.H.F., Covino, E., Alcalá, J.M., & Torres, G. 2001, *A&A*, 378, 898  
 Mermilliod, J.-C., Rosvick, J. M., Duquennoy, A., & Mayor, M. 1992, *A&A*, 265, 513  
 North, P., & Zahn, J.-P. 2003, *A&A*, 405, 677  
 Rieutord, M. 2004, *Stellar Rotation (IAU Symp. 215)*, ed. Ph. Eennens & A. Maeder, in press  
 Rocca, A. 1989, *A&A*, 213, 114  
 Savonije, G.J., & Witte, M.G. 2002, *A&A*, 386, 111  
 Scharlemann, E.T. 1982, *ApJ*, 253, 298  
 Stahler, S.W. 1983, *ApJ*, 274, 822  
 Stahler, S.W. 1988, *ApJ*, 332, 804  
 Terquem, C., Papaloizou, J.C.B., Nelson, R.P., & Lin, D.N.C. 1998, *ApJ*, 502, 788  
 Verbunt, F., & Phinney, E.S. 2001, *A&A*, 296, 709  
 Willems, B., van Hoolst, T., & Smeyers, P. 2003, *A&A*, 397, 973  
 Witte, M.G., & Savonije, G.J. 1999a, *A&A*, 341, 842  
 Witte, M.G., & Savonije, G.J. 1999b, *A&A*, 350, 129  
 Witte, M.G., & Savonije, G.J. 2002, *A&A*, 386, 222  
 Zahn, J.-P. 1966a, *Annales Ap*, 29, 313  
 Zahn, J.-P. 1966b, *Annales Ap*, 29, 489  
 Zahn, J.-P. 1975, *A&A*, 41, 329

- Zahn, J.-P. 1977, A&A, 57, 383  
Zahn, J.-P. 1989, A&A, 220, 112  
Zahn, J.-P., & Bouchet, L. 1989, A&A, 223, 112